

# Atomic-scale imaging of polarization switching in an (anti-)ferroelectric memory material: Zirconia ( $\text{ZrO}_2$ )

S. Lombardo<sup>1</sup>, C. Nelson<sup>2</sup>, K. Chae<sup>3,4</sup>, S. Reyes-Lillo<sup>5</sup>, M. Tian<sup>6</sup>, N. Tasneem<sup>7</sup>, Z. Wang<sup>7</sup>, M. Hoffmann<sup>8</sup>, D. Triyoso<sup>9</sup>, S. Consiglio<sup>9</sup>, K. Tapily<sup>9</sup>, R. Clark<sup>9</sup>, G. Leusink<sup>9</sup>, K. Cho<sup>4</sup>, A. Kummel<sup>3</sup>, J. Kacher<sup>1</sup>, A. Khan<sup>1,7</sup>  
<sup>1</sup>MSE, Georgia Tech; <sup>2</sup>Oak Ridge National Lab; <sup>3</sup>Chem., MSE., UCSD; <sup>4</sup>MSE, UT Dallas; <sup>5</sup>Physical Sciences, U. Chile, Chile;  
<sup>6</sup>IEN, Georgia Tech; <sup>7</sup>ECE, Georgia Tech; <sup>8</sup>NaMLab/Tu Dresden, Germany; <sup>9</sup>TEL Technology Center, America, LLC, USA.

Email: slombardo6@gatech.edu; akhan40@gatech.edu

**Abstract:** Direct, atomic-scale visualization of polarization switching in a functional, polycrystalline, binary oxide via *in-situ* high-resolution transmission electron microscopy (HRTEM) biasing is reported for the first time. Antiferroelectric (AFE)  $\text{ZrO}_2$  was used as the model system, which is important for commercial DRAMs and as emerging NVMs (through work-function engineering). We observed (1) clear shifting and coalescing of domains within a single grain, and (2) dramatic changes of the atomic arrangements and crystalline phases—both at voltages above the critical voltage measured for AFE switching. Similar synergistic *in-situ* structural-electrical characterization can pave the way to understand and engineer microscopic mechanisms for retention, fatigue, variability, sub-coercive switching and analog states in ferroelectric and AFE-based memory devices.

**Introduction:** There are significant gaps in our fundamental understanding of (poly-/nano-)crystalline nature of ALD  $\text{HfO}_2/\text{ZrO}_2$ -based ferroelectric(FE)/anti-ferroelectric oxides [1]. Most importantly, because polarization is coupled to the crystal structure, the application of a voltage/electric field changes the microscopic features *e.g.* grain orientation, phase, size and sub-grain characteristics (interphase boundaries and domain walls). Such dynamic evolution of microstructural features enables electrical characteristics *e.g.* multi-level cell (MLC) for embedded NVM [2] and poses significant challenges for *very large-scale integration* (VLSI) such as variation, reliability and endurance [3,4,5]. The first step towards quantitative structural-electrical correlation is the direct imaging of polarization switching at the atomic and mesoscopic scales with applied bias. In the present study, we probed electric field-induced structural changes with atomic-scale resolution through *in-situ* HRTEM in a polycrystalline functional, binary oxide. As a model system, we utilized AFE  $\text{ZrO}_2$ , which can enable NVM through work-function engineering with competitive—and in some metrics (*e.g.*, endurance) better—features than their FE counterparts [6].

**Results:** An ALD grown  $\text{TiN}(10\text{nm})/\text{ZrO}_2(10\text{nm})/\text{TiN}$  MIM structure was annealed at 450°C in  $\text{N}_2$ . After electrical characterization, the top TiN electrode was etched, and the sample bonded to a sacrificial Si substrate, diced, and double-side polished. After mounting to a Cu TEM grid, the Si was ion milled, exposing the sample film with an approximate final thickness between 50-100 nm. *In-situ* biasing was performed in an FEI Titan spherical aberration-corrected TEM-STEM and probe-based Nanofactory TEM sample biasing holder, with step voltages applied between 0 and 4V (Fig. 1). A probe tip diameter of approximately 10-20 nm allowed for precise contact and local biasing of individual  $\text{ZrO}_2$  grains.

To confirm the parent phase at 0 V, a nano-beam electron diffraction (NBED) scan over 0.5  $\mu\text{m}$  along the  $\text{ZrO}_2$  layer was performed in which an electron diffraction pattern (DP) was

collected from each grain and a summed DP was generated (Fig. 2a). A single pattern from this scan was isolated and found to be a close match to the simulated DP of a DFT-calculated [7] [111]-oriented tetragonal  $P4_2/nmc$  structure (Fig. 2b-c). NBED intensity was extracted from the summed DP and compared to the electron diffraction intensities of tetragonal  $P4_2/nmc$  and polar, orthorhombic  $Pca2_1$  phases (Fig. 2). The  $P4_2/nmc$  phase intensity is a strong match compared to the experimental. At higher  $1/d$ , some features of the  $Pca2_1$  phase intensity are also observed in the experimental, suggesting a minute presence of this FE phase at 0V, in agreement with the small opening in the AFE hysteresis loop shown in Fig. 4.

An individual  $\text{ZrO}_2$  grain was *in-situ* probed (Fig. 3) with bias sequence: 0 → 2V → ... 4V → ... 2V → 0V and correlated with the characteristic  $P$ - $V$  double hysteresis loop, cycled up to  $10^7$  cycles (Fig. 4). At 0V, the grain had 3 domains *visually* evident from the different orientations of the atomic planes (Fig. 5A). With increased bias, the right most domain expanded squeezing the middle domain—completely engulfing it at 4V. During the bias up-sweep, dramatic changes began to occur between 2-3V, which was also the on-set of macroscopic polarization switching observed in the  $P$ - $V$  loop. The microstructures returned to the original 3-domain pattern as the bias was reduced to 0V. However, the domain structure did not follow the same path during the bias up- and down-sweep which was the consistent with the AFE hysteresis (see domain patterns at 3V in fig. 5C and 5F).

Zoomed-in images of the same area obtained from the HRTEM images show a rectangular arrangement of Zr atoms (Fig. 6). When 0V images are superimposed with Zr atoms along the (112) projection (which is perpendicular to the growth direction, *i.e.*, [111]) of the tetragonal  $P4_2/nmc$  phase, an excellent (but not necessarily unique) match is observed (Fig. 7). When voltage is applied, a ‘sudden’ appearance of additional face-centered atoms in half of the rectangles occurs, indicating a partial phase transformation (Fig. 8b). Suggested (but not unique) atomic arrangements of the two phases at 4V are shown in Fig. 8. These changes were observed in each subsequent cycle (*i.e.*, 0V → 4V → 0V → 4V, Fig. 9).

**Conclusions:** We studied micro-structural evolution during polarization switching in AFE  $\text{ZrO}_2$  via *in-situ* HRTEM probing. Our study is the first of its kind for fluorite-type binary FEs/AFEs that can provide correlation between structural and electrical features for understanding and engineering the microscopic mechanisms behind fatigue, retention, endurance, reliability and variability, sub-coercive switching, analog states and so on for VLSI memory applications.

**Acknowledgements:** This work was supported by ASCENT, one of six JUMP centers, an SRC program sponsored by DARPA, and the SRC GRC program. A part of the work was conducted at CNMS, a DOE Office of Science User Facility.

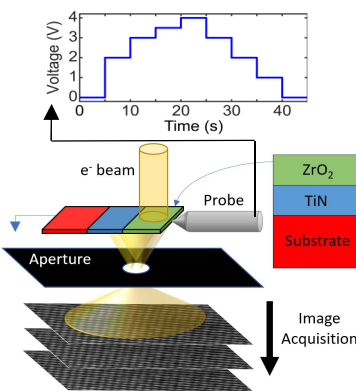


Fig. 1. In-situ voltage applied over time (top) and in-situ HRTEM sample probing schematic of AFE ZrO<sub>2</sub> thin films (bottom).

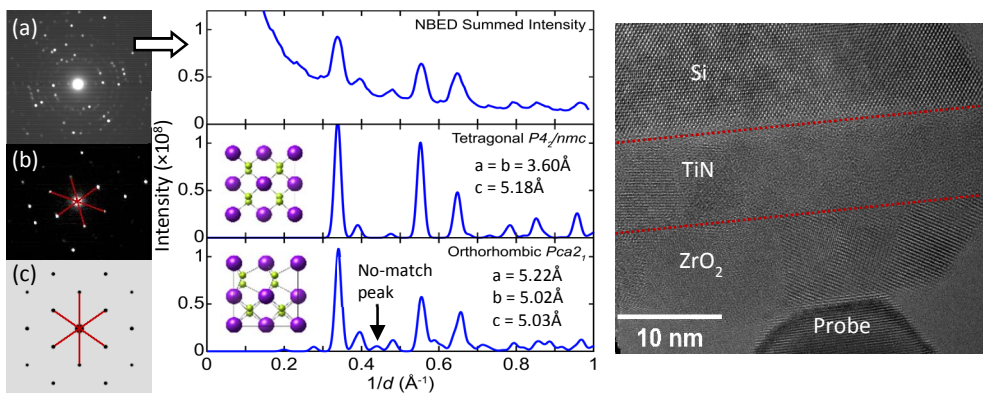


Fig. 2. Summed NBED pattern (a), experimental diffraction pattern (DP) from a single grain (b), a simulated tetragonal DP oriented along the [111] direction (c). Experimental, simulated tetragonal, and simulated orthorhombic electron diffraction intensity-1/d ( $\text{\AA}^{-1}$ ) curves (right).

Fig. 3. HRTEM of in-situ probing of a single grain in a 10nm polycrystalline ZrO<sub>2</sub> thin-film with a 10nm TiN bottom electrode over a Si substrate.

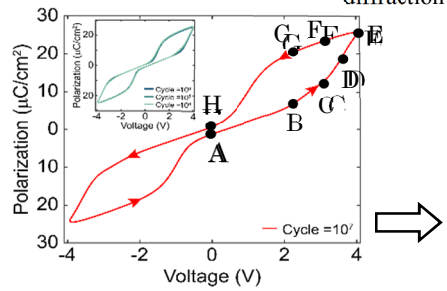


Fig. 4. Characteristic polarization-voltage hysteresis curve of the TiN(10nm)/ZrO<sub>2</sub>(10nm) TiN(10nm) capacitor showing AFE double-hysteresis loops after  $10^7$  cycles, with black dots (A-H) indicating applied voltages during *in-situ* HRTEM probing.

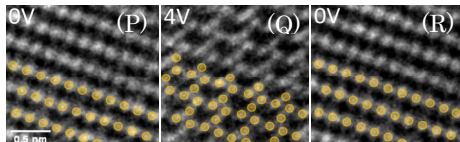


Fig. 6. Zoomed-in images of the same region in the right-most domain in the HRTEM snapshots indicated by rectangles in Fig. 8 at the initial 0V (P), 4V (Q), and final 0V (R) bias, with atomic positions highlighted.

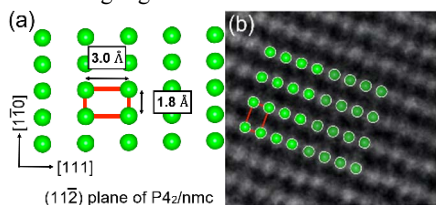


Fig. 7. Atomic model of (11-2) projected plane of the P4<sub>2</sub>/nmc phase (a) superimposed onto the HRTEM image of the right-most domain at 0V (b).

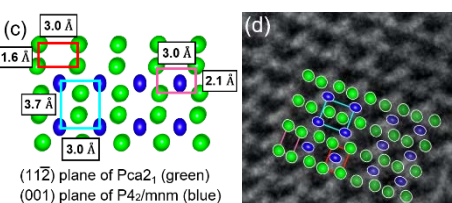


Fig. 8. Atomic model of (11-2) projected plane of the Pca<sub>2</sub>1 phase and (001) projected plane of the P4<sub>2</sub>/mnm phase (a) superimposed onto the HRTEM of the right-most domain at 0V (b).

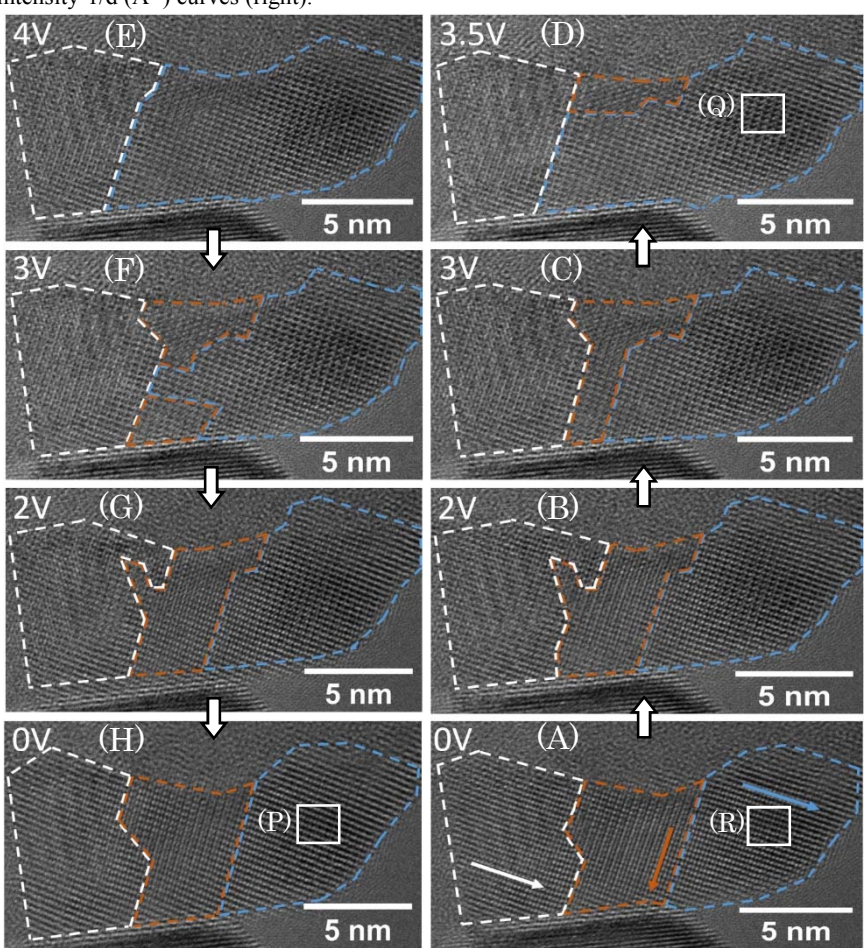


Fig. 5. In-situ HRTEM images captured while bias is applied through the probe in the sequence:  $0 \rightarrow 2\text{V} \rightarrow \dots 4\text{V} \rightarrow \dots 2\text{V} \rightarrow 0\text{V}$ .

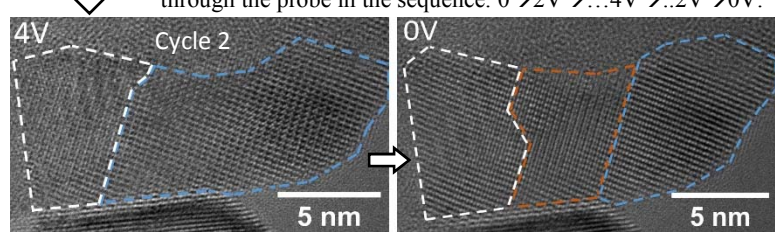


Fig. 9: HRTEM images of the AFE ZrO<sub>2</sub> grain at 0V and +4V for the second cycle.

**References:** [1] Muller et al. NanoLett. 12, 4318 (2012). [2] Mulaosmanovic et al. IEDM 26.8.1 (2015). [3] Ni et al. VLSI Symp., T40 (2019). [4] Pešić et al. Adv. Func. Mater. 26, 4601 (2016). [5] Grimley et al. Adv. Mater. Int. 5, 1 (2018). [6] Pešić et al. IEDM 11-6 (2016). [7] Reyes-Lillo et al. PRB 90, 140103 (2014).